Analytical and Bioanalytical Chemistry
https://doi.org/10.1007/s00216-020-02833-z

RESEARCH PAPER

On-spot quantitative analysis of dicamba in field waters using a lateral flow immunochromatographic strip with smartphone imaging

Meng Qi[1,2] · Jingqian Huo[1] · Zhenfeng Li[2] · Cong He[1] · Dongyang Li[2] · Yuxin Wang[2] · Natalia Vasylieva[2] · Jinlin Zhang[1] · Bruce D. Hammock[2]

Received: 9 June 2020 / Revised: 11 July 2020 / Accepted: 17 July 2020

Abstract

Dicamba herbicide is increasingly used in the world, in particular, with the widespread cultivation of genetically modified dicamba-resistant crops. However, the drift problem in the field has caused phytotoxicity against naive, sensitive crops, raising legal concerns. Thus, it is particularly timely to develop a method that can be used for on-the-spot rapid detection of dicamba in the field. In this paper, a lateral flow immunochromatographic strip (LFIC) was developed. The quantitative detection can be conducted by an app on a smartphone, named "Color Snap." The tool reported here provides results in 10 min and can detect dicamba in water with a LOD (detection limit) value of 0.1 mg/L. The developed LFIC shows excellent stability and sensitivity appropriate for field analysis. Our sensor is portable and excellent tool for on-site detection with smartphone imaging for better accuracy and precision of the results.

Keywords Dicamba · Smartphone-based sensor · On-site rapid detection

Introduction

Dicamba is an efficient, economic, and broadleaf herbicide, commonly used in corn, triticeae crops, and pastures. It is also largely used for weed control in dicamba-resistant (DR) soybean, corn, and DR cotton [1, 2]. Moreover, dicamba has excellent herbicidal effects. According to soybean growers, using dicamba can effectively remove weeds [3]. Since first introduced to the market in 1996, genetically modified (GM) soybeans have been cultivated in leading soybean exporting countries such as the USA, Brazil, and Argentina [4]. Especially in the USA, 94% of the soybean were GM varieties in 2017 [5]. The large-scale cultivation of GM varieties has greatly increased the use of dicamba. However, dicamba may cause injury to neighboring off-target plants by herbicide volatilization [6–8]. According to studies in Arkansas, Tennessee, Missouri, Indiana, and Nebraska, dicamba can volatilize and transferred to non-target areas [9], causing phytotoxicity to some crops that are sensitive to dicamba, such as tomato (*Solanum lycopersicum* L.), watermelon (*Citrullus lanatus* (Thunb.) Matsum. & Nakai), alfalfa (*Medicago sativa* L.), dry beans (*Phaseolus vulgaris* L.), peanut (*Arachis hypogaea* L.), grape (*Vitis* spp.), as well as noncultivated vegetation [10–14]. At the same time, the dicamba affects human health; a higher level of dicamba may increase the potential of hepatic tumors, cause DNA-damage, and also result in cytotoxicity and genotoxicity [15–17]. Gonzalez et al. found that 200 μg/mL dicamba can significantly induce the exchange of sister chromosomes, and 500 μg/mL dicamba cannot only cause cell poisoning but also affect the cell cycle process [18]. To support responsible product stewardship, it is essential to develop a convenient and effective detection method for dicamba monitoring in the field water, helping correct the misuse of this important herbicide.

Meng Qi and Jingqian Huo contributed equally to this work.

✉ Jinlin Zhang
zhangjinlin@hebau.edu.cn

✉ Bruce D. Hammock
bdhammock@ucdavis.edu

[1] College of Plant Protection, Hebei Agricultural University, Baoding 071001, Hebei, China

[2] Department of Entomology and Nematology and UCD Comprehensive Cancer Center, University of California, Davis, CA 95616, USA

Published online: 31 July 2020

Currently, the tracking of dicamba is mainly performed with large equipment-based technologies, such as LC-MS/MS [19], UPLC-MS/MS [20], and GC-MS/MS [21]. These analytical methods, however, require highly trained professional and expensive instruments. Enzyme-linked immunosorbent assay (ELISA) is another promising detection method used for dicamba analysis due to its overwhelming advantages in high sensitivity, speed, excellent selectivity, simplicity, low cost, high throughput, and no need of complicated pretreatment procedures. Clegg et al. developed an ELISA method for the detection of dicamba with a limit of detection (LOD) of 2.3 ng/mL and an IC_{50} (analyte concentration causing a 50% inhibition of the maximum response) of 195 ng/mL [22]. Huo et al. developed a chemiluminescent ELISA (CLEIA) for the detection of dicamba using novel hapten design. The IC_{50} was decreased as low as 0.874 ng/mL [23]. However, ELISA still is a laboratory-based method requiring special instruments, and this is not suitable for on-site monitoring. To tackle this issue, lateral flow immunochromatographic strip (LFIC) tests appear to be a promising solution due to their instrument-free feature, portability, and rapidness (usually within 15 min to produce results) [24]. This method has been widely used in the qualitative detection of pesticides and some other small molecules [25–29]. So far, there has been no LFIC available for the detection of dicamba. There is urgent need to develop LFICs for on-spot detection of dicamba for regulators and farms involved. However, it is worth noting that the LFIC has its intrinsic drawback as a qualitative or semi-quantitative assay; many strategies aiming at digital reading of the strips have been proposed to overcome this problem. For example, Zhuang Tian et al. and Kamlesh Shrivas et al. used ImageJ, a free Java-based software developed by the National Institute of Health of United States for image processing and analysis, to develop methods for detecting 19-nortestosterone and iron (III), respectively [30, 31]. Based on similar principle, Li et al. used the smartphone app called Color Grab to achieve the quantitative detection of test strips [32]. However, this software modification is only applicable to Android-based phones, which limits the scope of application of this detection method. Recently, a free smartphone app called Color Snap developed by Sherwin-Williams Company is suitable for a variety of mobile phone systems. It provides an online network version, which has broader prospects for use. This app can pick RGB data from the image and is often used in interior design. To date, no one has reported that the software can be used for visual inspection of the lateral flow immunochromatographic strips. As the Color Snap app allows users to capture the desired colors on their smartphone and then match those colors to interior design [33, 34], it is theoretically possible to digitally read a lateral flow immunochromatographic strip with a smartphone and quantify the concentration of analyte.

In this work, using the anti-dicamba polyclonal antibody previously produced against novel hapten [23], we developed a lateral flow immunochromatographic strip for dicamba monitoring with Color Snap app combined to image the strips. The goal of on-spot quantitative detection of dicamba in the field water was achieved.

Materials and methods

Chemicals and reagents

Bovine serum albumin (BSA), ovalbumin (OVA), potassium carbonate, and chloroauric acid solution were obtained from Sigma (St. Louis, MO). Protein-G columns and goat anti-rabbit IgG were supplied by Solarbio Corporation (Beijing, China). Nitrocellulose (NC) films were purchased from Sartorius (Gottingen, Germany). Polyester fiber membranes, special absorbent paper, plastic cards, and glass fiber (GF) membranes were bought from Shanghai Kinbio Tech Co., Ltd. (Shanghai, China). Serum and coating antigen were developed in a previous study [23]. Standards (dicamba; 5-hydroxydicamba; 2,3,5-trichlorobenzoic acid; 2,3,6-trichlorobenzoic acid; clopyralid; picloram; chloramben and chlorfenac) were obtained from Thermo Fisher Scientific (Rockford, IL), Sigma-Aldrich (St. Louis, MO) or Chem Service, Inc. (West Chester, PA). The solvents and reagents used in this study were all of analytical grade.

Preparation of the nanogold particles

Gold nanoparticles (AuNPs) were prepared according to ref. [35]. In brief, 1.0 mL 1% (w/v) $HAuCl_4$ solution was diluted with 100 mL Milli-Q water in a flat-bottom flask and heated until boiling. Then, 2.25 mL of sodium citrate solution (1%) was one time added to the flask with continuous stirring. After about 2 min of boiling, the color of the solution changed from purple to wine-red, and it continued to boil for another 15 min. The heat was turned off, and the solution continued until it cooled down to the room temperature (RT). The volume of the solution was adjusted to the original volume by Milli-Q water. Resulting nanogold suspension was characterized by a UV-visible spectrum at whole wavelengths. The solution was stored at 4 °C until used.

Preparation of the antibody-nanogold probe

The serum against dicamba was obtained in a previous work [23]. Polyclonal serum was purified by protein-G columns. The antibody concentration was determined with a NanoDrop spectrophotometer. Then the antibody was determined by an ELISA using the homologous and heterologous coating antigens in separate assays. The steps of ELISA were

performed according to the ref. [23]. In brief, a microtiter plate was coated with heterologous/homologous coating antigen (100 μL/well) overnight at 4 °C and blocked with 3% skim milk (200 μL/well). After the plate was washed three times, dicamba standard and an equal volume antibody solution (50 μL/well) were added. Then goat anti-rabbit IgG–horseradish peroxidase (100 μL/well in 10,000 dilution) was added after five times wash. Then TMB-substrate solution was added after washing five times. Finally, the reaction was stopped by H_2SO_4, and the absorbance was read at 450 nm.

Before conjugation, the optimal pH value for the nanogold suspension was determined as follows: different volumes of 0.1 M K_2CO_3 solution were added to 100 μL of nanogold suspension, followed by the addition of the purified antibody. After brief mixing, the solution was left at RT for 1 h. Then 10 μL 10% NaCl was added, mixed, and left at RT for another 1 h. The color change and precipitation of the solution were observed. Finally, the above-mixed solutions were placed in a transparent 96-well plate, and the absorbance was measured at 520 nm by a UV spectrophotometer. Conditions providing maximum absorbance value were considered as optimal. Similarly, the optimal amount of antibody was adjusted by changing the concentration of antibody in the reaction system to obtain a high signal to noise and linearity.

Based on the above results, 0.1 M K_2CO_3 solution was added to 10 mL of nanogold suspension under gentle stirring, followed by the purified antibody, and the solution was continuously stirred for 30 min. After adding 800 μL of 10% (w/v) bovine serum albumin (BSA) solution for blocking, stirring continued for 20 min. Then the solution was centrifuged for 15 min at 2000 rpm at 4 °C. Resulting supernatant contained gold nanoparticles conjugated with antibody (Ab-NP), while unconjugated gold particles were collected as a pellet. Thus, the supernatant was transferred in a clean vial and centrifuged for 30 min at 10,000 rpm to separate conjugated gold nanoparticles from free antibody and BSA. The pellet was washed twice by resuspending in a buffer (contain 0.05% BSA, 0.05% PVP, 1.2% Tris, and 1.0% Tween 20, pH 9.0) followed by centrifugation. Finally, the pellet was resuspended in 50 μL of buffer (contain 0.05% BSA, 0.05% PVP, 1.2% Tris, and 1.0% Tween 20, pH 9.0) and stored at 4 °C for further use.

Preparation of the lateral flow immunochromatographic strip

The lateral flow immunochromatographic strip was composed of five parts. The NC film, conjugate pad, sample pad, and absorbent pad were glued on the PVC board in superposing layers (Fig. 1a), then cut into strips of 4 mm wide, and stored for later use (RT). The concentration of coating antigen, antibody-nanogold probe, and goat anti-rabbit IgG was optimized, respectively. The coating antigen and goat anti-rabbit IgG were coated on the NC film as detection line (T-line) and control line (C-line), while the antibody-nanogold probe was soaked onto a conjugate pad. As shown in Fig. 1b once the sample is applied to a sample pad, it migrates across the layers toward the absorption pad due to capillary forces. If the sample solution contains dicamba, the free dicamba will compete with the coating antigen on T-line for the binding of antibody-nanogold probe. When the concentration of dicamba is high, all the Ab-NP will bind the dicamba, and no binding will occur on the T-line. Thus, no color will be observed on the test line. Absent test line or faint test line corresponding to lower dicamba concentration are positive read-out and valid, as long as control line is observed too. The concentration of dicamba in the sample solution is inversely proportional to the color of T-line. The C-line is coated with species-specific antibody capturing anti-dicamba antibody. It should always turn red during analysis to prove the validity of the test strip. Otherwise, the test strip is invalid.

To obtain the lateral flow immunochromatographic strip with the best sensitivity several parameters had to be optimized. Then the coating antigen concentration was optimized

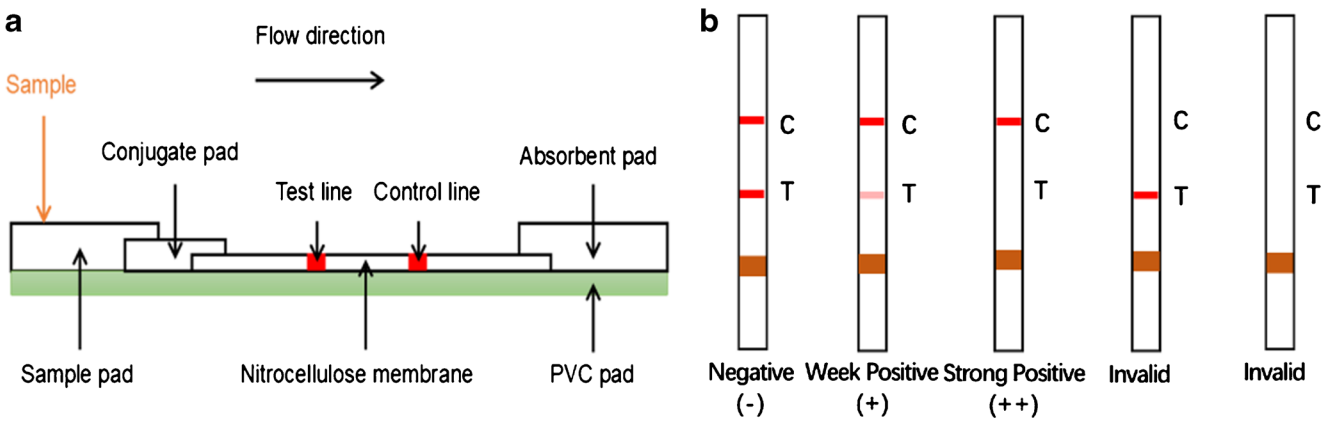

Fig. 1 The principle and structural composition of immunochromatographic test strip (**a**) and the judgment criteria of immunochromatographic test strip by naked eye (**b**)

by diluting to 0.08, 0.20, 0.40, 0.50, 0.80, 1.33, and 2.0 mg/L with carbonate buffer (pH 9.6) and then coating onto NC membranes as the T-line. The antibody-nanogold probe was diluted to 2-, 4-, and 8-fold with 0.01 M phosphate-buffered saline (PBS, pH 7.2), then coated to the conjugate pad. The goat anti-rabbit IgG was diluted to 0.1, 0.2, 0.5, 0.8, 1.0, and 2.0 mg/mL with 0.01 M PBS (pH 7.2), then coated onto NC membranes as the C-line. The coating conditions were optimized by setting serial conditions, three coating temperatures for 4, 25, 37 °C and four coating time for 0.5, 1, 2, and 16 h. And then seven kinds of buffers (0.01 M PBS buffer pH 7.2, **1**; 0.01 M PBS buffer pH 7.2 containing 0.1% BSA and 0.15% Tween 20, **2**; 0.01 M PBS buffer pH 7.2 containing 10% BSA, **3**; 0.01 M PBS buffer pH 7.2 containing 0.1% BSA, **4**; 0.01 M PBS buffer pH 7.2 containing 0.15% Tween 20, **5**; 0.01 M PBS buffer pH 7.2 containing 0.05% Tween 20, **6**; Milli-Q water pH 7.2, **7**) were prepared for conjugate pad and five kinds of buffers (0.01 M PBS pH 7.2, **1**; 0.01 M PBS buffer pH 7.2 containing 1% BSA and 0.25% Tween 20, **2**; 0.01 M PBS buffer pH 7.2 containing 1% BSA, **3**; 0.01 M PBS buffer pH 7.2 containing 0.25% Tween 20, **4**; Milli-Q water pH 7.2, **5**) for use on the sample pad, to get the best sensitivity.

The judgment criteria by naked eye were as follows: the antibody-nanogold probe in the conjugate pad was totally released, the sample solution crosses the whole strip, T-line and C-line turn red clearly for the negative samples "–," T-line fade clearly for the strong positive "++," and turn faint red for weak positive "+."

Quantitative detection of dicamba with Color Snap on smartphone

Quantitative detection of dicamba is achieved by analyzing high-quality photos using the Color Snap app. The specific experimental steps are as follows: (1) Use a smartphone equipped with a Color Snap application to take a photo of the test strip in a well-lit place or use a flashlight from smartphone in a low light situation. (2) Make the T-line in the middle of the picture by cropping the picture size. (3) Open the Color Snap and select "Match a Photo," then click on the lower-left corner to load the image. (4) Touch the screen to enlarge the picture as much as possible, while keeping the C-line and T-line in the center of the screen, then click "done." (5) Click the trash can icon in the lower-left corner to delete all preset color recognition until the icon is invisible, then tap the "+" put the circle to the C-line and T-line. (6) Tap the color name and get the RGB value for C-line and T-line. And the gray-scale value for C-line and T-line is calculated from the RGB value by the following formula [36]:

$$\text{Gray} = R \times 0.3 + G \times 0.59 + B \times 0.11$$

(7) In order to reduce the influence of background color on the gray-scale value, the T-line gray-scale value, C-line gray-scale value, and the ratio of T-line gray-scale value to C-line gray-scale value in the same strip (T/C value) were compared under different light intensity. The influence of background on the detection result can be effectively reduced when the T/C value was selected as the stable parameter instead of the T-line gray-scale value scanning signal, which is also consistent with the reported research [37, 38]. Then use the free App "WPS office" on the smartphone to draw a standard curve with different concentrations of dicamba as the abscissa and the T/C values as ordinate to achieve quantitative detection (in order to achieve true and sensitive test results, each on-site test should redraw the standard curve to adapt to the environmental conditions). (8) Then the limit of detection (LOD) value was calculated according to the ICH (International Conference on Harmonization of Technical Requirements for Registration of Pharmaceuticals for Human Use) guideline criteria as 3.3σ/slope, where σ is the standard deviation of the blank measurements (no dicamba in sample solution, $n = 6$) [39].

Specificity and stability of the lateral flow immunochromatographic strip

The specificity of the lateral flow immunochromatographic strip was evaluated by using a set of dicamba structural analogs, including 5-hydroxydicamba; 2,3,5-trichlorobenzoic acid; 2,3,6-trichlorobenzoic acid; clopyralid; picloram; and chloramben and chlorfenac. Then the lateral flow immunochromatographic strips were used to detect the sample solutions of the above compounds with different concentrations. Through the color change of T-line, the naked eye test results of each compound were obtained. Then the T/C values of each concentration were obtained by the Color Snap app.

The stability of the lateral flow immunochromatographic strip was evaluated by comparing the sensitivity of different batches of the strip and the sensitivity of the same batch stored at 4, 25, and37 °C for 180 days. The sample solution of dicamba at 0.250 mg/L was used to perform analysis every 15 days. The validity of the test strip was judged by the naked eye and comparing the test concentration obtained by the strip analysis with the phone.

Analysis of the spiked sample

Irrigation water and river water were collected to use in evaluation studies. The irrigation water was collected in the field in which dicamba was never used before. The river water was collected from the river near the field. All the water samples were confirmed by LC-MS to be free from dicamba. Every spiked concentration in each matrix was tested in six

replicated. For validation of the precision and repeatability of the method, and according to the published literature, the concentration of dicamba may vary in different conditions. Vance et al. [40] found the concentration of dicamba in soil-water was 0.31–0.46 mg/L after 2 weeks of use and became lower than 0.0015 mg/L 96 days after application when dicamba was used at low dose (0.9 kg/ha). At the same time, the investigation results by Ensminger et al. [41] on surface water and sediment pesticides in mid-California showed that the concentration of dicamba in the urban surface water sample was 0.06–119 μg/L. Grover et al. [42] investigated the herbicide residues in farm dugouts and ponds, and it showed that the concentration of dicamba remaining in the water samples in the Merford area was 11.7 μg/L. Therefore, three different concentrations of dicamba solution (the final concentration was 0.05, 0.15, and 0.30 mg/L) were added to the sample solution with the same volume. The strip test was run in a blind fashion, and Color Snap was used for color analysis to obtain the T/C value. The concentration of dicamba in the sample was quantitatively analyzed according to the established calibration curve.

Results and discussion

Characterization of the nanogold particles

The quality of the antibody-nanogold probe is one of the main factors affecting the lateral flow immunochromatographic strip. The size of nanogold particles is affected by the amount of trisodium citrate. Although some researches have suggested that the suitable diameter of nanogold particles for coupling maybe 30–40 nm, some scholars also have developed a highly sensitive detection method with the 20 nm nanogold particles [43–46]. In this research, 2.25 mL of trisodium citrate solution (1%) was used in the preparation of the nanogold particles. The nanogold particle suspension was a pink uniform liquid observed by naked eyes, and the solution was scanned at 459–600 nm by an ultraviolet-visible spectrophotometer. The results showed that there was a unique maximum absorbance peak at 520 nm. The scanning results of transmission electron microscopy (TEM) of the nanogold particles showed that the size of nanogold particles was a relatively uniform 20 nm (Fig. 2).

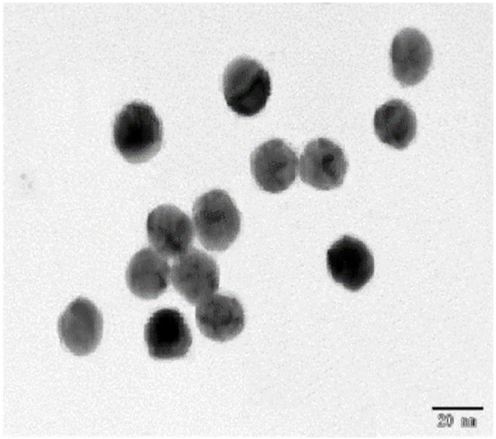

Fig. 2 The transmission electron microscopy (TEM) image of the prepared nanogold particles with the diameter of approximately 20 nm

Preparation of the antibody-nanogold probe

The purified antibody was obtained by using protein-G columns to purify the serum and confirmed activities by ELISA, and the concentration of the antibody was 3.0 mg/mL. Based on previous research results, a high concentration antibody may not be suitable for the preparation of the antibody-nanogold probe [47]. The antibody was diluted to 2.5 mg/mL before conjugation. When the nanogold particles were mixed with the purified antibody in different buffers for conjugation, the unstable antibody-nanogold probe will precipitates with the addition of 10% NaCl, while the stable probe will maintain a uniform solution state and has high absorbance at 520 nm. Therefore, the optimum pH value and amount of antibody were determined by measuring the absorbance of the solution at 520 nm wavelength. The maximum absorption at 520 nm was observed when 30 μL of 0.1 M K_2CO_3 was added to 100 μL of particles. At these conditions, the pH value of the solution was 9 (Fig. 3a). This indicates that pH 9.0 is optimal for adsorption of polyclonal antibody to the nanogold particles. With these conditions, no precipitation of nanoparticles occurred at 10% NaCl. Then the minimum amount of antibody was determined in the same way. The maximum absorption at 520 nm was observed with 30 μL of 2.5 mg/mL antibody added to 100 μL of nanoparticles, resulting in final concentration of 0.75 mg/mL (Fig. 3b). Previous studies have shown that the chosen concentration of antibody must be greater than the minimum antibody for best performance in LFIC, and usually, the optimal antibody concentration for probe binding is 1.1 times of the minimum amount of antibody [48]. So, the final concentration of antibody binding was 0.825 mg/mL (0.75 mg/mL plus 1.1-fold).

Based on the results above, the antibody and nanogold particle suspension is coupled by electrostatic interaction to obtain a stable antibody-nanogold probe [49]. Then, the antibody-nanogold probe was characterized by a UV spectrophotometer at different wavelengths. As shown in Fig. 3c, due to the increase in the particle size of the conjugation after the antibody binds to nanogold particles, the maximal absorption peak shifted from 520 to 530 nm. This peak shift phenomenon means that the antibody has been coupled with nanogold particles successfully [50].

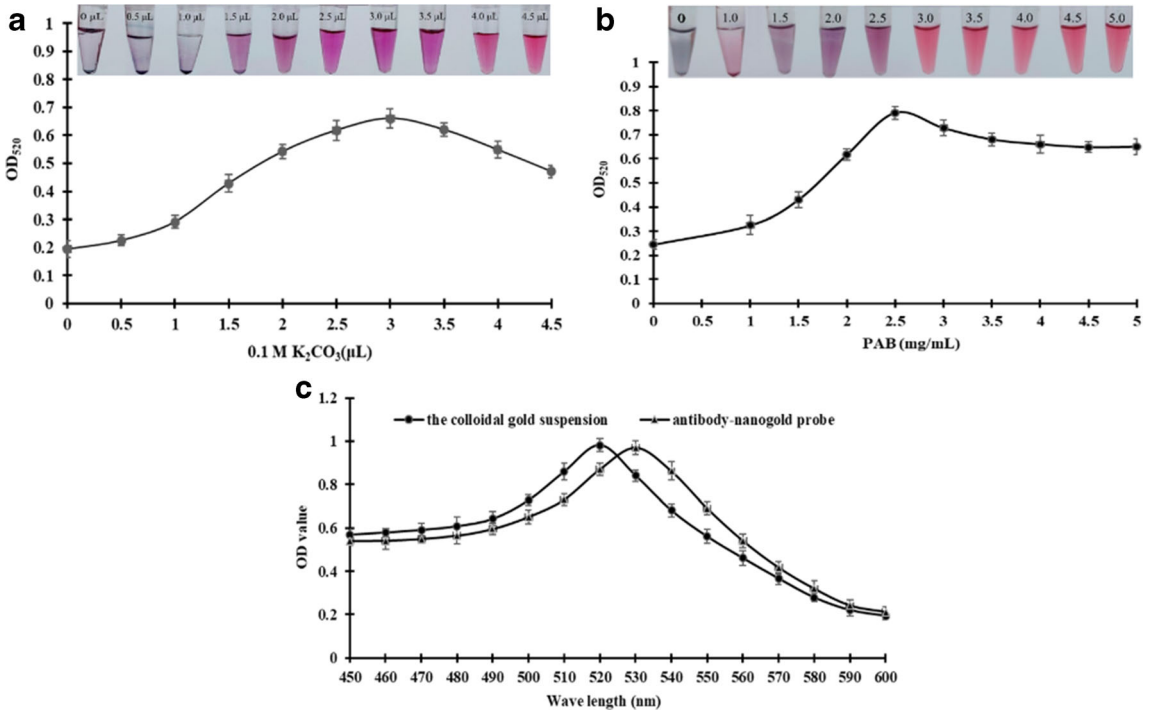

Fig. 3 Absorbance curve for the optimization determination of pH value (**a**) and antibody amount (**b**) in the preparation of the antibody-nanogold probe; the *x*-axis represents the concentration of K_2CO_3 and the antibody amount, and the *y*-axis represents the mean value of absorbance (520 nm). The optical density (OD) values of nanogold particles and antibody-nanogold probe at different wavelengths (**c**)

Preparation of the lateral flow immunochromatographic strip

In the present study, to obtain the immunochromatographic test strip with the best sensitivity, the proper amount of coating antigen, antibody-nanogold probe, goat anti-rabbit IgG, coating conditions, buffers for conjugate pad, and buffers for the sample were optimized. The naked eye was applied for the judgment criteria for LFIC preparation and optimizing as the naked eye is more intuitive, convenient, and fast and the results have a consistent trend while comparing with the app imaging and calculation procedure.

First, one factor was set as a variable, and other factors were kept constant. The optimal value of each variable was screened one by one by this method. In the absence of dicamba, the best result where the T-line turn red clearly was observed when the homologous coating antigen was diluted to 0.8 mg/L and the antibody-nanogold probe was diluted to 2-fold. It was determined that the best concentration of goat anti-rabbit IgG was 1.0 mg/mL. The optimal coating conditions were 25 °C for 30 min. The best blocking buffers for conjugate and the sample pads were 0.01 M PBS buffer (pH 7.2) containing 0.1% BSA and 0.15% Tween 20 and 0.01 M PBS (pH 7.2) containing 1% BSA and 0.25% Tween 20, respectively. Several rounds of optimization were cycled through to approach optimum conditions.

Therefore, the conjugate pads, sample pads, antibody-nanogold probe, coating antigens, and goat anti-rabbit IgG were prepared with the conditions above. The lateral flow immunochromatographic test strip was finished after each part of the test strip was assemble and then cut the strips into 4 mm, stored for later use (4 °C).

The sensitivity of the lateral flow immunochromatographic strip by Color Snap on smartphone

Based on the previous polyclonal antibody ELISA results and the concentration of dicamba in environment from previous studies [23, 40, 41], a series of different concentrations of dicamba solution (0, 0.050, 0.100, 0.150, 0.200, 0.250, and 0.300 mg/L) were tested using the test strips. The results indicated that the T-line became lighter with the increase of dicamba and the T-line began to fade when the concentration of dicamba was 0.100 mg/L until it disappeared completely at 0.300 mg/L (Fig. 4a). So, the naked eye limit of dicamba was 0.300 mg/L.

Then the Color Snap application on a smartphone was used for C-line and T-line's RGB value detection. The gray-scale value of C-line and T-line were calculated by using RGB value, then T/C value was obtained as the ratio of both lines' gray-scale values. With increasing concentration of dicamba, the T-line becomes lighter until it disappears, while the C-line remains red. Since gray-scale value is inversely related to color intensity, thus, the gray-scale value of the T-line gradually increases as the concentration of dicamba increases (Fig.

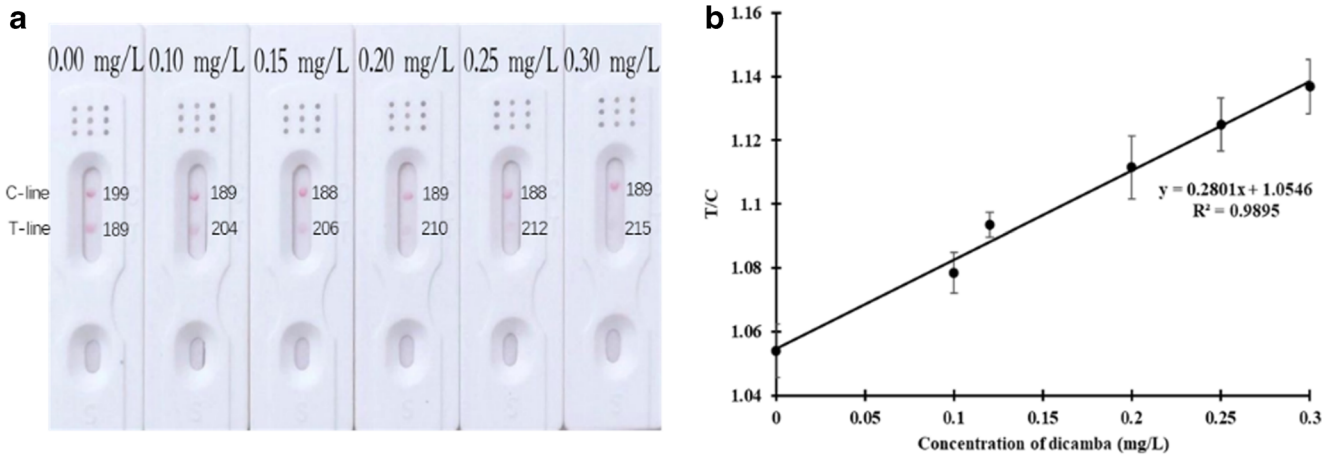

Fig. 4 Test strip test results of dicamba solution tested at different concentrations, the T-line became lighter with the increase of dicamba, and T-line began to fade when the concentration of dicamba was 0.100 mg/L until it disappeared completely at 0.300 mg/L; the gray-scale values of T-line and C-line were marked in (**a**). The calibration curve is drawn by Color Snap, the *x*-axis represents the concentration of dicamba, and *y*-axis represents the T/C value (the ratio of T-line gray-scale value to C-line gray-scale value in the same strip under the same shooting conditions) (**b**)

4a); therefore, the T/C value was positively correlated with dicamba concentration. And the results of T/C values and the gray-scale value of T-line and C-line were compared with the naked eye evaluation (Table 1). T/C value was inversely proportional to the color of the T-line observed by the naked eye, but directly proportional to the concentration of dicamba. The concentration of dicamba is used as the horizontal axis and the T/C values as the vertical axis to draw a calibration curve (Fig. 4b). Although the signal change is not dramatic, it is consistent and correlates with the concentration of the analyte. The calibration curve has a good linear relationship between the concentration of dicamba and T/C values in the range of 0–0.300 mg/L ($R^2 = 0.9895$). The LOD (detection limit) value was 0.1 mg/L. Based on the obtained standard curve, quantitative detection of dicamba can be achieved.

In the immunoassay against small molecules, the coating antigen is a key component of competitive format. Generally, the antibodies have a better binding with the homologous coating antigen. However, the free analyte will be more easily displaced from the heterologous antigen providing higher sensitivity of the assay. In an indirect competitive ELISA format based on antibodies against dicamba, the LOD of 0.013 mg/L with homologous pair is higher than that with heterologous pair (0.0015 mg/L) (Fig. 5a). However, when we applied the heterologous coating antigen in LFIC, the binding of polyclonal antibody conjugated nanogold particle was too weak to form an obvious T-line (Fig. 5b). Therefore, we switched back to the homologous pair for LFIC. Though the sensitivity of our developed LFIC (LOD = 0.1 mg/L) was six times lower than homologous ELISA, this sensitivity is still applicable for field monitoring studies. It indicated that the affinity was not lost after antigen/antibody immobilization, as it is often observed that lateral flow assay is less sensitive than classical ELISA. It might be due to the much faster interaction during

Table 1 The results by Color Snap for dicamba detection

Sample number	Concentration (mg/L)	Naked eye	Gray-scale value		Color Snap (T/C)
			T-line	C-line	
1	0	+++	199	189	1.054
2	0.100	++	204	189	1.078
3	0.150	+	206	188	1.094
4	0.200	+	210	189	1.112
5	0.250	−	212	188	1.125
6	0.300	−−	215	189	1.137

T/C the ratio of T-line gray-scale value to C-line gray-scale value in the same strip under the same conditions, the gray-scale value of T-line and C-line were calculated by using RGB value obtained from Color Snap

−−: there is no color at all, −: there is almost no color, +: the color is lighter, ++: the color is appropriate, +++: the color intensity of the analyte is strong and has a great contrast with the background

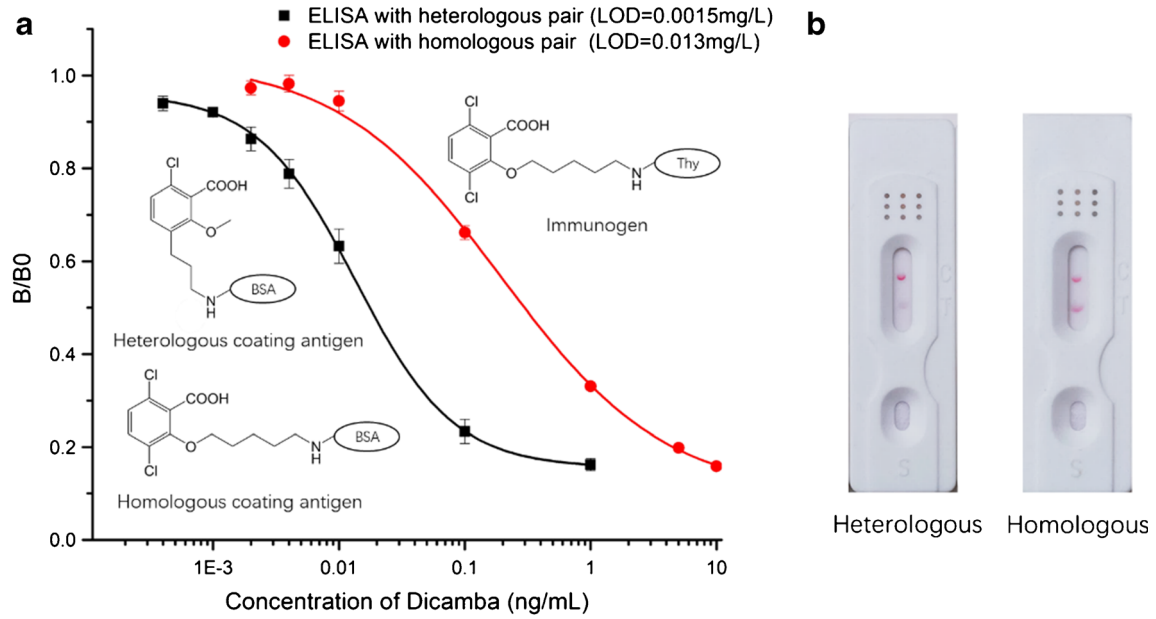

Fig. 5 Inhibition curve for dicamba using antibodies. Immunogen (JQ-00-24–Thy), homologous coating antigen (JQ-00-24–BSA), heterologous coating antigen (JQ-00-21–BSA), and goat anti-rabbit-IgG –horseradish peroxidase, 1:10000. Each point was tested in triplicate (**a**), and the LFICs used the heterologous coating antigen and homologous coating antigen as the T-line (**b**)

the flow and there is not time for proper equilibrium that is reached in plate-based assay and the conjugation of the antibody to the particle might affect the antibody binding [51–55].

Due to the lower sensitivity, the developed LFIC is not suitable for determining the low dicamba concentration in soil or plant samples. Since the LOD value of LFIC (0.1 mg/L) is lower than the maximum acceptable concentration (MAC) for dicamba in drinking water (0.120 mg/L) [15], the sensitivity of LFIC is suitable for detecting the water sample. At the same time, LFIC has the advantage of being fast and portable. And we creatively combined the smartphone imaging with the LFIC technology to conquer for the drawback of traditional LFICs; the upgraded LFIC is successfully applied for on-spot quantitative analysis in the field. If the tested field water is positive of dicamba by LFIC, it indicates that the illegal use of dicamba is happening, and then our previous assay with better sensitivity will be applied for the further soil and plant testing. This two-step procedure can be used to reduce the workload of sample collection then leading to the rational use of monitoring dicamba. To monitor the illegal use of dicamba in the field, we set up a two-step monitoring procedure: the environmental water sample was first screened on-spot with the LFIC quickly in the field; if dicamba positive sample was found, the soil and plant in the same area were collected and determined in the laboratory.

The specificity of the lateral flow immunochromatographic strip

The developed test strips were evaluated by a set of dicamba structural analogs to examine the selectivity of LFIC. And the concentrations were set as follows: 0, 0.100, 0.150, 0.200, 0.250, 0.300, 0.500, and 1.0 mg/L. The T/C values of each compound at this concentration were calculated respectively, dicamba and the blank (no dicamba or other analyte) have the highest and lowest T/C value separately. And all the other compounds except 2,3,6-trichlorobenzoic acid maintained the lower T/C values compared with the dicamba and similar with the blank, indicating that the test strip had good selectivity to dicamba with no cross-reactivity to these structural analogs (Fig. 6). The 2,3,6-trichlorbenzoic acid has lower T/C value compared with dicamba, but with a relatively higher number compared with the blank. It indicates that this analog has slight cross-reactivity in LFIC for dicamba. However, 2,3,6-trichlorobenzoic acid is not widely used as herbicide currently and is unlikely to be found in field water samples. This result is consistent with the previous studies [23]. Therefore, these results show that the test strip reported here has good specificity for the detection of dicamba.

Stability of the lateral flow immunochromatographic strip

The stability of the tool was characterized by testing different batches of the developed strips under and the same batch stored at different conditions. Three batches of test strips were prepared to analyze a sample solution with a concentration of 0.250 mg/L as shown in Table 2. All the LFICs of different batches were reproducible for the detection of the dicamba at fixed concentration. The

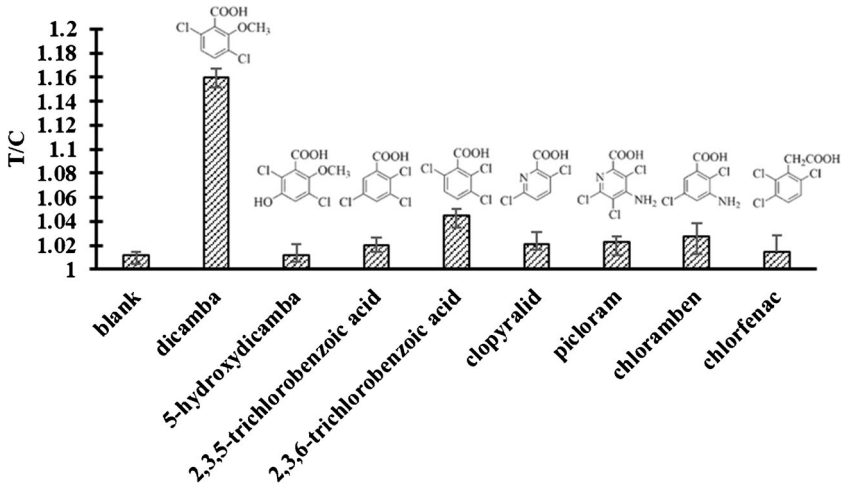

Fig. 6 Cross-reactivity of the developed test strips against dicamba structural analogs. The *x*-axis represents the solution of dicamba or dicamba structural analogs and the concentration was 1.0 mg/L (blank represents no dicamba or other analyte), and the *y*-axis represents the T/C value

developed test strips provide reproducible results for 180 days when stored at 4 °C, 75 days when stored at 25 °C, and 15 days when stored at 37 °C (data not shown). It indicated that the strip performance directly correlated with storage temperature. The result showed that the shelf life of the test strips was longer under the low temperature. This observation is most probably due to the fact that protein reagents used in test strip preparation preserve their activity and properties better at low temperature [50]. Therefore, the optimum storage condition was 4 °C. We monitored the strips up to 180 days.

Analysis of the spiked sample

The developed strips were designed for on-site detection of dicamba in the field. Irrigation water and river water were collected to evaluate the matrix effect in dicamba the detection and quantification. First, all the water samples were confirmed to be free from dicamba by LC-MS. Then a series of dicamba solution (0, 0.100, 0.150, 0.200, 0.250, 0.300, 0.500, and 1.0 mg/L) were diluted by PBS buffer and water sample (diluted 0-, 10-, and 100-fold in the PBS buffer) respectively, and tested with the developed test strip under the same conditions. The results show that the results of undiluted water samples were similar to PBS buffer (data not shown). So, these water samples have almost no matrix effect and can be directly used for detection. Then the detection was carried out with the spiked water samples by the addition of known dicamba concentration (the final concentration was 0.050, 0.150, and 0.300 mg/L). The spiked water samples were analyzed by the developed test strip. As shown in Table 3, the average recovery rate from three water samples using the developed test strip was from 95.6 to 103.1%. The relative standard deviations were 1.5 to 4.4%, indicating that the LFIC method is accurate and reliable.

This showed that the developed test strip could effectively detect the dicamba in environmental water samples without further purification and treatment. The previous studies have shown that because dicamba is highly water soluble, stable to chemical hydrolysis, and highly mobile [56, 57], it can enter the atmosphere by drift, evaporation, sublimation, or soil erosion and then return in the form of

Table 2 Stability of different batches of test strips ($n = 3$)

Batch	Found (mg/L)	CV (%)	Naked eye
1	0.242	2.15	–
2	0.251	3.33	–
3	0.247	1.51	–

The samples solutions containing 0.250 mg/L dicamba. – –: there is no color at all, −: there is almost no color, +: the color is lighter, ++: the color is appropriate, +++: the color intensity of the analyte is strong and has a great contrast with the background

Table 3 The test result of the spiked recovery test ($n = 6$)

Sample	Spiked (mg/L)	Found (mg/L)	Recovery (%)	CV (%)
Irrigation water	0.050	0.049	98.5	4.4
	0.150	0.155	103.1	2.6
	0.300	0.296	98.6	3.0
River water	0.050	0.049	98.2	1.5
	0.150	0.149	99.2	4.0
	0.300	0.287	95.6	2.1

The water samples were added with dicamba standard, and the final concentration of dicamba was 0.050, 0.150, and 0.300 mg/L. The concentration of dicamba were analyzed by the developed test strip

rainfall [58]. Ensminger et al. analyzed water samples from surface water in California; among the 225 samples, more than 40% of the samples detected dicamba, and the number of positive sample and concentration of dicamba detected in the water samples increased significantly when the rainfall increased [41]. On the other hand, Willett et al. have shown that dicamba dissolved in irrigation water can cause damage to dicamba-sensitive soybeans [59]. The test strip developed can quickly detect the water samples in field and monitor the use of dicamba.

Conclusion

Lateral flow immunochromatographic strip for dicamba quantification was successfully developed. This strip can quickly and easily detect the dicamba in the field water. These data can be used to estimate the dicamba drift in the field. In addition, without complicated instruments, the quantitative analysis of dicamba can be achieved by analyzing the RGB value of the test strip image using a free smart mobile phone application Color Snap. This low-cost and portable test strip is sensitive with a detection limit for dicamba in the water of 0.1 mg/L. The LOD was lower than dicamba contamination possible in soil-water and surface water [40, 41]. This assay was successfully applied in the quantitative analysis of dicamba spiked in the field water. This tool could provide guidance on the rational use of dicamba in the field. It also provides a tool to deal with legal concerns about dicamba drift.

Funding information This work was financially supported by the National Institute of Environmental Health Science Superfund Research Program (P42ES004699), the National Nature Science Foundation of China (No. 31871981), Graduate Research and Innovation Program of Hebei (CXZZBS2019099), the National Nature Science Foundation of Hebei (No. C2020204116) and the National Academy of Sciences (NAS, Subaward no. 2000009144). The article is derived from the subject data funded in part by NAS and USAID and opinions, findings, conclusions, or recommendations expressed in this article are those of the authors alone and do not necessarily reflect the views of USAID or NAS.

Compliance with ethical standards

All procedures involving animals were approved and performed in accordance with the relevant protective and administrative guidelines for laboratory animals of China.

Conflict of interest The authors declare that they have no conflict of interest.

References

1. Jones GT, Norsworthy JK, Barber T. Off-target movement of diglycolamine dicamba to non-dicamba soybean using practices to minimize primary drift. Weed Technol. 2019;33(1):24–40.
2. Shaner D L. Herbicide handbook. Weed Science Society of America. Lawrence; 2014.
3. Werle R, Oliveira MC, Jhala AJ, Proctor CA, Rees J, Klein R. Survey of Nebraska farmers' adoption of dicamba-resistant soybean technology and dicamba off-target movement. Weed Technol. 2018;32(6):754–61.
4. Lee TC, Edrington TC, Bell E, Burzio LA, Glenn KC. Effect of common processing of soybeans on the enzymatic activity and detectability of the protein, dicamba mono-oxygenase (DMO), introduced into dicamba-tolerant MON 87708. Regul Toxicol Pharmacol. 2019;102:98–107.
5. James C. Global status of commercialized biotech/GM crops in 2017: Biotech crop adoption surges as economic benefits accumulate in 22 years. ISAAA Brief No. 53.: The International Service for the Acquisition of Agri-biotech Applications (ISAAA); 2017.
6. Sciumbato AS, Chandler JM, Senseman SA, Bovey RW, Smith KL. Determining exposure to auxin-like herbicides. I. Quantifying injury to cotton and soybean. Weed Technol. 2004;18(4):1125–34.
7. Behrens R, Lueschen W. Dicamba volatility. Weed Sci. 1979;27(5):486–93.
8. Grover R, Maybank J, Yoshida K. Droplet and vapor drift from butyl ester and dimethylamine salt of 2, 4-D. Weed Sci. 1972;20(4):320–4.
9. Jones GT, Norsworthy JK, Barber T, Gbur E, Kruger GR. Off-target movement of DGA and BAPMA dicamba to sensitive soybean. Weed Technol. 2019;33(1):51–65.
10. Bruns V. The response of certain crops to 2, 4-dichlorophenoxyacetic acid in irrigation water: part I. Red Mexican Beans Weeds. 1954;3(4):359–76.
11. Culpepper AS, Sosnoskie LM, Shugart J, Leifheit N, Curry M, Gray T. Effects of low-dose applications of 2, 4-D and dicamba on watermelon. Weed Technol. 2018;32(3):267–72.
12. Egan JF, Bohnenblust E, Goslee S, Mortensen D, Tooker J. Herbicide drift can affect plant and arthropod communities. Agric Ecosyst Environ. 2014;185:77–87.
13. Hill B, Harker K, Hasselback P, Moyer J, Inaba D, Byers S. Phenoxy herbicides in Alberta rainfall: potential effects on sensitive crops. Can J Plant Sci. 2002;82(2):481–4.
14. Johnson VA, Fisher LR, Jordan DL, Edmisten KE, Stewart AM, York AC. Cotton, peanut, and soybean response to sublethal rates of dicamba, glufosinate, and 2, 4-D. Weed Technol. 2012;26(2):195–206.
15. Caux P-Y, Kent R, Tache M, Grande C, Fan G, MacDonald D. Environmental fate and effects of dicamba: a Canadian perspective. In: Reviews of environmental contamination and toxicology. New York Springer 1980. pp. 1–58.
16. Perocco P, Ancora G, Rani P, Valenti A, Mazzullo M, Colacci A, Grilli S. Evaluation of genotoxic effects of the herbicide dicamba using in vivo and in vitro test systems. Environ Mol Mutagen. 1990;15(3):131–5.
17. Reuter W (2019) Toxicology of glyphosate, isoxaflutole, dicamba and possible combination effects. Testbiotech https://doi.org/www.testbiotech.org/sites/default/files/Tox_Evaluation_Glyphosate_Dicam ba_Isoxaflutole.pdf Accessed 18.
18. González N, Soloneski S, Larramendy M. Genotoxicity analysis of the phenoxy herbicide dicamba in mammalian cells in vitro. Toxicol in Vitro. 2006;20(8):1481–7.
19. Xiong W, Tao X, Pang S, Yang X, Tang G, Bian Z. Separation and quantitation of three acidic herbicide residues in tobacco and soil by dispersive solid-phase extraction and UPLC–MS/MS. J Chromatogr Sci. 2014;52(10):1326–31.
20. Sturm J, Wienhold P, Frenzel T, Speer K. Ultra Turrax® tube drive for the extraction of pesticides from egg and milk samples. Anal Bioanal Chem. 2018;410(22):5431–8.
21. Guo H, Riter LS, Wujcik CE, Armstrong DW. Quantitative analysis of dicamba residues in raw agricultural commodities with the use of

ion-pairing reagents in LC–ESI–MS/MS. Talanta. 2016;149:103–9.
22. Clegg BS, Stephenson GR, Hall JC. Development of an enzyme-linked immunosorbent assay for the detection of dicamba. J Agric Food Chem. 2001;49(5):2168–74.
23. Huo JQ, Barnych B, Li ZF, Wan DB, Li DY, Vasylieva N, Knezevic SZ, Osipitan OA, Scott JE, Zhang JL, Hammock BD. Hapten synthesis, antibody development, and a highly sensitive indirect competitive chemiluminescent enzyme immunoassay for detection of dicamba. J Agric Food Chem. 2019;67(20):5711–9. https://doi.org/10.1021/acs.jafc.8b07134.
24. Thobhani S, Attree S, Boyd R, Kumarswami N, Noble J, Szymanski M, Porter RA. Bioconjugation and characterisation of gold colloid-labelled proteins. J Immunol Methods. 2010;356(1–2):60–9.
25. Li Q, Liu L, Chen W, Peng C, Wang L, Xu C. Gold nanoparticle-based immunochromatographic assay for the detection of 7-aminoclonazepam in urine. Int J Environ Anal Chem. 2009;89(4):261–8.
26. Li H, Sun B, Chen T. Detection of clothianidin residues in cucumber and apple juice using lateral-flow immunochromatographic assay. Food Agric Immunol. 2019;30(1):1112–22.
27. Song S, Suryoprabowo S, Liu L, Kuang H, Xu L, Ma W, Wu X. Development of monoclonal antibody-based colloidal gold immunochromatographic assay for analysis of halofuginone in milk. Food Agric Immunol. 2019;30(1):112–22.
28. Chen Z, Wu X, Xu L, Liu L, Kuang H, Cui G. Development of immunocolloidal strip for rapid detection of pyrimethanil. Food Agric Immunol. 2019;30(1):1239–52.
29. Zhang X, Liu L, Cui G, Song S, Kuang H, Xu C. Preparation of an anti-isoprocarb monoclonal antibody and its application in developing an immunochromatographic strip assay. Biomed Chromatogr. 2019;33(11):e4660.
30. Tian Z, Liu LQ, Peng C, Chen Z, Xu C. A new development of measurement of 19-nortestosterone by combining immunochromatographic strip assay and ImageJ software. Food Agric Immunol. 2009;20(1):1–10.
31. Shrivas K, Kant T, Karbhal I, Kurrey R, Sahu B, Sinha D, et al. Smartphone coupled with paper-based chemical sensor for on-site determination of iron (III) in environmental and biological samples. Anal Bioanal Chem. 2020;412(7):1573–83.
32. Li Q, Ren S, Peng Y, Lv Y, Wang W, Wang Z, et al. A colorimetric strip for rapid detection and real-time monitoring of histamine in fish based on self-assembled PDA vesicles. Anal Chem. 2019;92(1):1611–7.
33. Urban GL, Sultan F. The case for 'Benevolent' mobile apps. MIT Sloan Manag Rev. 2015;56(2):31.
34. Ricci L. Immersive media and branding: how being a brand will change and expand in the age of true immersion. In: Handbook of research on the global impacts and roles of immersive media: IGI Global; 2020. pp. 393–414.
35. Liu X, Xiang JJ, Tang Y, Zhang XL, Fu QQ, Zou JH, et al. Colloidal gold nanoparticle probe-based immunochromatographic assay for the rapid detection of chromium ions in water and serum samples. Anal Chim Acta. 2012;745:99–105. https://doi.org/10.1016/j.aca.2012.06.029.
36. Bala R, Braun KM. Color-to-grayscale conversion to maintain discriminability. Electronic Imaging 2004. SPIE. 2003;5293:196–202.
37. Di Nardo F, Alladio E, Baggiani C, Cavalera S, Giovannoli C, Spano G, Anfossi L. Colour-encoded lateral flow immunoassay for the simultaneous detection of aflatoxin B1 and type-B fumonisins in a single test line. Talanta. 2019;192:288–94.
38. Li X, Wang J, Yi C, Jiang L, Wu J, Chen X, Shen X, Sun Y, Lei H. A smartphone-based quantitative detection device integrated with latex microsphere immunochromatography for on-site detection of zearalenone in cereals and feed. Sensors Actuators B Chem. 2019;290:170–9.
39. Siangdee N, Youngvises N. Smart sensor using cellulose-based material for TNT detection. Key Eng Mat. 2019;803:124–8.
40. Vance GF, Krzyszowska AJ. Monitoring dicamba and picloram movement and fate in the vadose zone for groundwater quality protection in Wyoming. The Center; 1994.
41. Ensminger MP, Budd R, Kelley KC, Goh KS. Pesticide occurrence and aquatic benchmark exceedances in urban surface waters and sediments in three urban areas of California, USA, 2008–2011. Environ Monit Assess. 2013;185(5):3697–710.
42. Grover R, Waite DT, Cessna AJ, Nicholaichuk W, Irvin DG, Kerr LA, Best K. Magnitude and persistence of herbicide residues in farm dugouts and ponds in the Canadian prairies. Environ Toxicol Chem. 1997;16(4):638–43.
43. Zeng L, Wu X, Liu L, Xu L, Kuang H, Xu C. Production of a monoclonal antibody for the detection of vitamin B 1 and its use in an indirect enzyme-linked immunosorbent assay and immunochromatographic strip. J Mater Chem B. 2020;8(9):1935–43.
44. Hu G, Gao S, Han X, Yang L. Comparison of immunochromatographic strips using colloidal gold, quantum dots, and upconversion nanoparticles for visual detection of norfloxacin in milk samples. Food Anal Methods. 2020;13:1069–77.
45. Zhou X, Wang M, Cheng A, Yang Q, Wu Y, Jia R, et al. Development of a simple and rapid immunochromatographic strip test for detecting duck plague virus antibodies based on gI protein. J Virol Methods. 2020;277:113803.
46. Dong S, Liu Y, Zhang X, Xu C, Liu X, Zhang C. Development of an immunochromatographic assay for the specific detection of Bacillus thuringiensis (Bt) Cry1Ab toxin. Anal Biochem. 2019;567:1–7.
47. Qiuyan T, Yunlong W. Practical techniques of immunodiagnostic reagents. China Ocean Press; 2009.
48. Chenggang S, Suqing Z, ZHANG K, Guobao H, Zhenyu Z. Preparation of colloidal gold immunochromatography strip for detection of methamidophos residue. J Environ Sci. 2008;20(11):1392–7.
49. Xiulan S, Xiaolian Z, Jian T, Zhou J, Chu F. Preparation of gold-labeled antibody probe and its use in immunochromatography assay for detection of aflatoxin B1. Int J Food Microbiol. 2005;99(2):185–94.
50. Hu W, Yan Z, Li H, Qiu J, Zhang D, Li P, et al. Development of a new colloidal gold immunochromatographic strip for rapid detecting subgroup A of avian leukosis virus using colloidal gold nanoparticles. Biochem Eng J. 2019;148:16–23.
51. Rong-Hwa S, Shiao-Shek T, Der-Jiang C, Yao-Wen H. Gold nanoparticle-based lateral flow assay for detection of staphylococcal enterotoxin B. Food Chem. 2010;118(2):462–6.
52. Ling S, Chen Q-A, Zhang Y, Wang R, Jin N, Pang J, Wang S. Development of ELISA and colloidal gold immunoassay for tetrodotoxin detetcion based on monoclonal antibody. Biosens Bioelectron. 2015;71:256–60.
53. Sun C, Liu L, Song S, Kuang H, Xu C. Development of a highly sensitive ELISA and immunochromatographic strip to detect pentachlorophenol. Food Agric Immunol. 2016;27(5):689–99.
54. Cho YA, Kim YJ, Hammock BD, Lee YT, Lee H-S. Development of a microtiter plate ELISA and a dipstick ELISA for the determination of the organophosphorus insecticide fenthion. J Agric Food Chem. 2003;51(27):7854–60.
55. Jin Y, Jang J-W, Han C-H, Lee M-H. Development of ELISA and immunochromatographic assay for the detection of gentamicin. J Agric Food Chem. 2005;53(20):7639–43.
56. Health & Human Sciences Research Institute. The Pesticide Properties DataBase (PPDB). Agriculture & Environment

Research Unit (AERU), University of Hertfordshire. 2013. http://hdl.handle.net/2299/15375. Accessed 15 Mar 2020.
57. Phillips PJ, Bode RW. Pesticides in surface water runoff in south-eastern New York State, USA: seasonal and stormflow effects on concentrations. Pest Manag Sci. 2004;60(6):531–43.
58. Hill BD, Harker KN, Hasselback P, Inaba DJ, Byers SD, Moyer JR. Herbicides in Alberta rainfall as affected by location, use and season: 1999 to 2000. Water Qual Res J. 2002;37(3):515–42.
59. Willett CD, Grantz EM, Lee JA, Thompson MN, Norsworthy JK. Soybean response to dicamba in irrigation water under controlled environmental conditions. Weed Sci. 2019;67(3):354–60.